American Mineralogist, Volume 78, pages 1181–1191, 1993

Coupled substitution of H and minor elements in rutile and the implications of high OH contents in Nb- and Cr-rich rutile from the upper mantle

Dimitrios Vlassopoulos
S. S. Papadopulos and Associates, Inc., 7944 Wisconsin Avenue, Bethesda, Maryland 20814-3620, U.S.A.
George R. Rossman
Division of Geological and Planetary Sciences, California Institute of Technology, Pasadena, California 91125, U.S.A.
Stephen E. Haggerty
Department of Geology, University of Massachusetts, Amherst, Massachusetts 01003, U.S.A.

Abstract

Infrared absorption spectra of rutile crystals from a variety of geological environments (carbonatite, hydrothermal vein, kyanite + rutile + lazulite association, xenoliths that are kimberlite hosted and dominated by Nb- and Cr-rich rutile) exhibit strong absorption in the 3300-cm^{-1} region due to interstitial protons bonded to structure O. In general the proton is located at sites slightly displaced from ½½0 of the unit cell, although some samples show evidence of additional protons at tetrahedral interstitial sites. H contents of rutile range up to 0.8 wt% H_2O, the highest concentrations occurring in mantle-derived Nb- and Cr-rich rutile of metasomatic origin. The role of H in rutile was examined, particularly with respect to its relations to other impurities. Protons are present in the rutile structure to compensate for trivalent substitutional cations (Cr, Fe, V, Al), which are only partly compensated by pentavalent ions (Nb, Ta). The possibility of using the H content of rutile as a geohygrometer is illustrated for the case of coexisting hematite and rutile.

Introduction

Rutile is known to have a great affinity for H, and therefore presents a unique opportunity for a case study of H incorporation mechanisms in nominally anhydrous minerals. Because of its industrial importance, there has been much effort directed toward understanding the defect chemistry of rutile, motivated by its special dielectric and optical properties, which have found use in numerous applications. The existence of structurally bound OH in rutile was first recognized by Soffer (1961). Since then several studies bearing on H in rutile and its effect on electrical and optical properties of synthetic as well as natural rutile have appeared (*vide infra*). Because the structural site and speciation of H in synthetic rutile is rather well constrained, a thermodynamic treatment of H in rutile is feasible, provided realistic reactions for H incorporation can be inferred from compositional relations among the various minor components present. In this study, we analyzed rutile in xenoliths from the upper mantle, carbonatite, kyanite quartzite (kyanite + rutile + lazulite association), and other geological environments and infer from the compositional systematics in natural rutile, in light of previous studies of its defect chemistry, the controls of H incorporation in rutile.

Previous work on structural OH in rutile

Soffer (1961) assigned a narrow double band near 3300 cm^{-1} in the infrared spectrum of pure Verneuil-grown crystals to an OH stretch mode. The study by von Hippel et al. (1962) suggested that there were two interstitial proton positions between O_a and O_b, each with a fourfold degeneracy (Fig. 1). This was reinterpreted by Johnson et al. (1968), considering the dichroicity of the OH absorption, which constrained the OH dipole axis to be in the basal (001) plane of the rutile structure. Johnson et al. (1968) considered the two possible sites that satisfied this requirement, ½½0 and ½00 (Fig. 1) and concluded that the ½00 site was energetically more favorable. The observed satellite peaks were reinterpreted as impurity-associated (Al, Ga, Ni, Mg) OH groups, suggesting that H plays a role as a charge compensator in trivalent cation doped rutile, in support of the suggestion of Hill (1968). Furthermore, Ohlsen and Shen (1974) and Andersson et al. (1973, 1974) found evidence from electron spin resonance and infrared spectra of Fe-doped rutile for Fe^{3+}-OH defect association, consistent with Fe^{3+} at the ½½½ Ti^{4+} site and the proton near the ½00 interstitial site. Johnson et al. (1968) were not able to resolve impurity-associated OH peaks in the infrared spectra of rutiles doped with Fe, Cr, and V and concluded that either there was no association of OH groups with these cations or the resultant shifts in the OH stretch band were too small to be detected.

Beran and Zemann (1971) reported the occurrence of a sharp absorption band at 3270 cm^{-1} due to OH groups in two rutile crystals. In a recent study, Hammer and

0003–004X/93/1112–1181$02.00

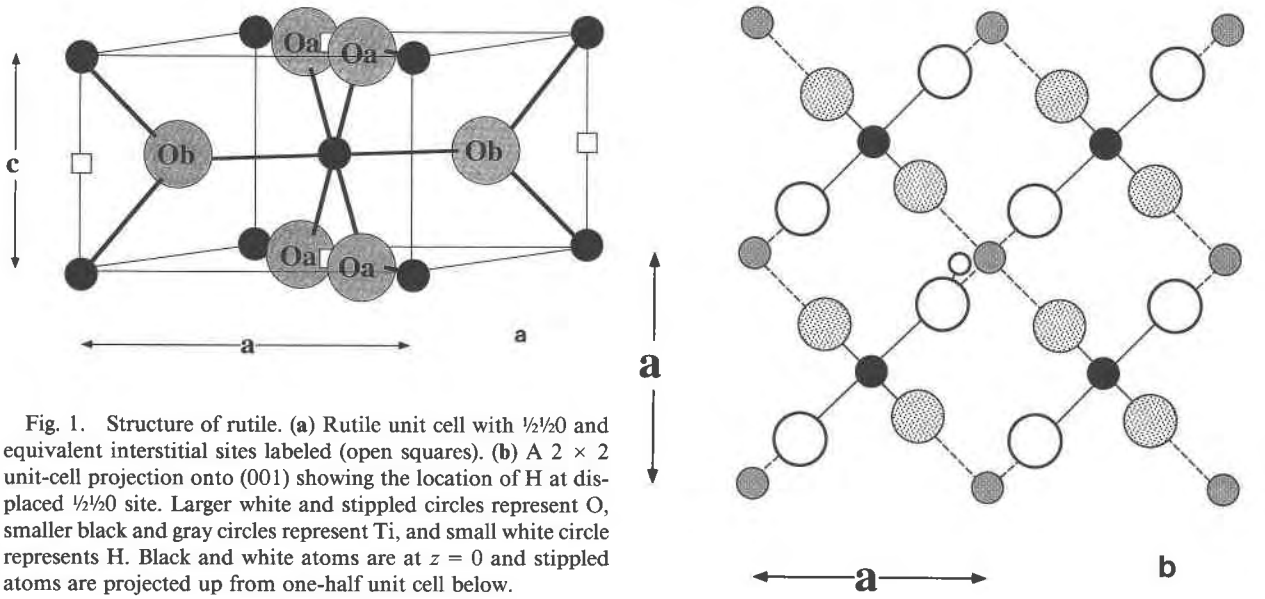

Fig. 1. Structure of rutile. (**a**) Rutile unit cell with ½½0 and equivalent interstitial sites labeled (open squares). (**b**) A 2 × 2 unit-cell projection onto (001) showing the location of H at displaced ½½0 site. Larger white and stippled circles represent O, smaller black and gray circles represent Ti, and small white circle represents H. Black and white atoms are at $z = 0$ and stippled atoms are projected up from one-half unit cell below.

Beran (1991) presented IR spectra of rutile from pegmatitic veins in mafic intrusives, fissures in low- to medium-grade metamorphic terrains, as well as high-pressure environments (eclogite and blueschist). This study established the widespread occurrence of OH in rutile of crustal origin. The rutile samples all exhibit a sharp band at 3280 cm^{-1}, and some show additional peaks at 3320 or 3360 cm^{-1}. The OH contents of the samples, determined from calibrated spectra, ranged from 0.04 to 0.2 wt% H_2O. The concentration of OH groups was found to be correlated with minor component concentration, and there was some indication that the environment of formation played a role in determining OH content.

Rossman and Smyth (1990) presented infrared spectra of Nb- and Cr-rich rutile from mantle eclogite xenoliths with surprisingly intense absorption peaks at 3300 and 3320 cm^{-1}, interpreted as being due to an elevated content of structural OH. A neutron diffraction study of a rutile crystal from the same sample (Swope et al., 1992) contributed the first direct evidence for the location of H in rutile. In contrast to the earlier studies of synthetic rutile, it was found that the H position was much closer to ½½0 than to ½00. Because of its implications, the discovery of elevated OH content in mantle rutile prompted the present study to examine additional mantle rutile from other associations in order to determine whether mantle rutile crystals are typically hydrous.

The eclogitic rutile studied by Rossman and Smyth (1990) contains an order of magnitude more OH (~0.7 wt% H_2O) than the eclogitic rutile of Hammer and Beran (1991) (0.08 wt% H_2O), suggesting that rutile from the two eclogite samples (1) equilibrated in significantly different physiochemical environments (e.g., H_2O activity, pressure, or temperature), (2) did not record equilibrium, or (3) equilibrated under similar conditions, but different amounts of OH were incorporated due to different minor element concentrations. The first possibility is likely, given that the xenoliths in the Roberts Victor kimberlite were entrained from the upper mantle, whereas the Dora Maira eclogites were formed at shallower depths. The second possibility is not as likely, since H readily diffuses through the rutile structure (Johnson et al., 1975). The third possibility is given credence by the fact that the less impure crystal had the lower OH content. It thus appears that a combination of physicochemical environmental conditions and the availability of substitutional cations must be responsible for variations in the OH content of natural rutile.

Materials and Methods

Polarized infrared absorption spectra and chemical compositions of both natural and synthetic single crystals of rutile were measured. The natural samples include rutile from a variety of geological settings: chlorite schist, kyanite quartzite deposits (aluminum silicate + rutile + lazulite association), hydrothermal vein, carbonatite, and kimberlite-hosted rutile-silicate and rutile-ilmenite nodules of upper mantle origin (Table 1). The synthetic samples consist of nominally pure and impurity-doped (Fe or Al) crystals.

The larger crystals were cut and polished into plates 0.03–1 mm thick oriented such that they contained the c axis parallel to the polished surfaces. The finer grained samples (aggregates of grains <1 mm in greatest dimension) were mounted on glass slides with thermoplastic cement prior to polishing the second side, and crystals of suitable orientation were subsequently located with a polarizing microscope.

Polarized infrared absorption spectra were obtained with a Nicolet 60SX Fourier-transform spectrophotometer using a $LiIO_3$ polarizer. Spectra were measured on regions of the samples that were free of fractures, inclu-

TABLE 1. Rutile samples studied

Sample	Locality	Association
	Natural	
R-1	Graves Mountain, GA	kyanite + rutile + lazulite
R-2	Graves Mountain, GA	kyanite + rutile + lazulite
R-4	Magnet Cove, AR	carbonatite
R-5	Polk County, TN	isolated crystal
R-6	PA-MD border	magnetite + apatite + chlorite schist
R-7	Namibia	hydrothermal vein
R-8	Pomfret, VT	hydrothermal vein
JAG83-30	Jagersfontein, South Africa	kimberlite-hosted rutile-ilmenite xenolith
JAG85-2	Jagersfontein, South Africa	kimberlite-hosted rutile-ilmenite xenolith
	Synthetic	
"Pure"	Commercial Crystal Laboratories, Naples, FL	
Al-doped	Commercial Crystal Laboratories, Naples, FL	
Fe-doped	Commercial Crystal Laboratories, Naples, FL	

sions, and other visible defects through pinhole apertures between 100 and 1000 μm in diameter. For mounted samples, the spectra were corrected for the effects of the glass slide and mounting medium by subtraction. Sample thicknesses in the region where the infrared spectra were taken were measured with a digital micrometer to ± 1 μm.

Selected samples were reacted with D_2O in a Teflon-lined pressure vessel (190 °C and saturated vapor pressure) or sealed in a Au capsule and placed in a rapid-quench cold-seal vessel (500 °C and 100 MPa) for 24 h. IR spectra were measured before and after deuteration to confirm that the peaks observed in unreacted samples were all due to OH vibrations.

Quantitative chemical analyses of the rutile samples were carried out with a Jeol 733 electron microprobe (15-kV accelerating voltage, 15-nA Faraday cup current) and on-line automated correction procedures. Prior to microprobe analysis the samples were screened on an X-ray fluorescence spectrometer in order to determine the minor elements present at detectable concentrations, as a guide in the selection of elements to be quantitatively analyzed.

RESULTS

IR spectroscopy

The polarized spectra confirm that the absorption features in the infrared region are intense and strongly pleochroic, the greatest absorption occurring when the electric vector (**E**) of the source radiation is polarized perpendicular to the crystallographic **c** axis of the sample.

The substitution of H by D in an OH harmonic oscillator results in the appearance of new absorption bands at $\nu_{OD} = \nu_{OH}/1.374$. As expected, new peaks in the IR spectra of partially deuterated samples appeared at $\nu_{OD} \approx \nu_{OH}/1.35$, confirming that all the features in the 3300-cm^{-1} region are due to OH.

The positions and relative intensities of the absorption bands in the region of 4000–2000 cm^{-1} are given in Table 2, and representative spectra are shown in Figure 2. The pure and Al-doped synthetic samples show a main peak at 3278 cm^{-1} and a satellite peak at 3324 cm^{-1}. After annealing at 1450 °C in air for 60 h, the Al-doped crystal showed an overall increase in absorbance, and the relative intensity of the satellite peak doubled. The Fe-doped crystal shows only the main band at 3278 cm^{-1} (Fig. 2a).

TABLE 2. IR absorption in rutile in the 3300-cm^{-1} region

Sample	ν_{OH} (cm^{-1})	Linear absorbance ⊥**c** (cm^{-1})*	Linear absorbance ∥**c** (cm^{-1})*	Integrated absorbance (cm^{-2})	H_2O (wt%)	H (pfu)
			Natural			
R-1	3290	32.9	—	4435.0	0.29	0.026
	3365	22.9	3.3			
R-2	3290	27.6	**	4756.0	0.31	0.027
	3365	24.0	**			
R-4	3290	10.6	—	1841.0	0.12	0.011
R-5	3290	9.5	—	1476.0	0.10	0.0085
R-6	3290	82.8	—	4260.0	0.28	0.025
R-7	3290	33.4	—	1775.0	0.12	0.010
R-8	3290	112.2	—	7381.0	0.48	0.043
JAG83-30-1	3290	133.3	—	8360.0	0.54	0.048
JAG83-30-2	3290	156.3	—	9233.0	0.60	0.053
JAG83-30-3	3290	185.3	—	12260.0	0.80	0.071
JAG85-2	3290	61.3	—	3844.0	0.25	0.022
			Synthetic			
Pure	3278	3.24	**	88.7	0.0057	0.0005
	3324	0.47				
Al-doped	3278	5.73	**	200.2	0.013	0.0012
	3324	2.20				
Fe-doped	3378	2.00	**	59.9	0.0039	0.0003

* Absorption intensity per centimeter for indicated polarization.
** The (001) section.

The IR absorption spectra of natural rutile crystals are broadly similar to those of the synthetic crystals, although satellite peaks are generally not resolved in spectra of natural rutile. The spectra typically show a single intense but broader band, with the peak at 3290 cm^{-1}. In two samples from Graves Mountain (R-1 and R-2), in addition to the peak at 3290 cm^{-1}, another broad peak at 3365 cm^{-1}, of subordinate intensity, was observed. Polarized spectra reveal that, in contrast to the dipole giving rise to the 3290-cm^{-1} peak, the orientation of the dipole causing this absorption is not confined to the basal plane (Fig. 2b).

The sample with the most intense absorption in the 3300-cm^{-1} region is JAG83-30, Nb- and Cr-rich rutile from a rutile-dominated xenolith from the Jagersfontein kimberlite, South Africa.

Calculation of H concentration in rutile

Calibrations of the infrared absorption intensity of the OH groups for estimating the H content in rutile have been presented by Johnson et al. (1973) and Hammer and Beran (1991). Johnson et al. (1973) determined a value of $\epsilon_{OH} = 15100 (\pm 500)$ L/(mol·cm^2) from D-H exchange experiments on synthetic rutile. Hammer and Beran

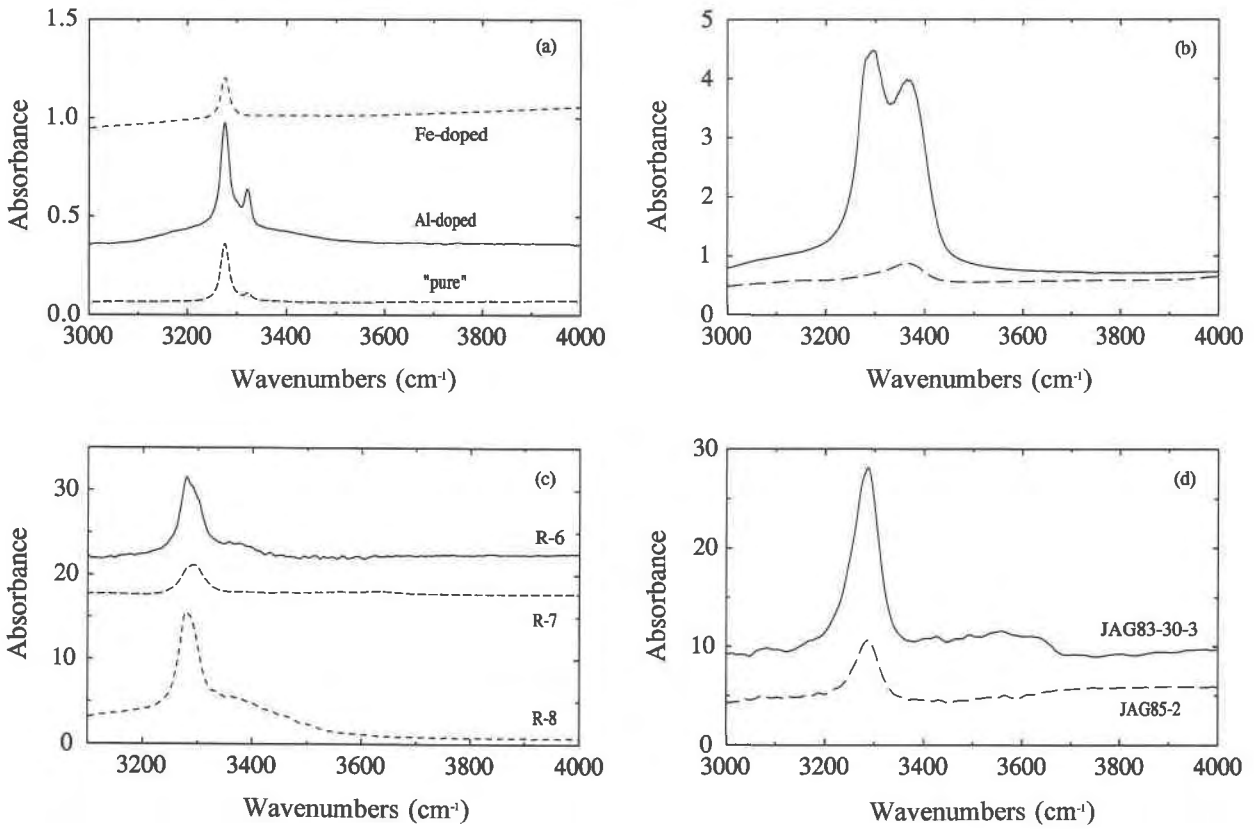

Fig. 2. Polarized IR spectra of rutile, plotted as 1000-μm sample thickness ($\mathbf{E} \perp \mathbf{c}$ in all spectra, except in **b**). (**a**) Synthetic rutile. Note absence of satellite peak at 3320 cm^{-1} in Fe-doped sample. (**b**) Rutile from kyanite + quartzite association (Graves Mountain), R-1. Solid line is for polarization $\mathbf{E} \perp \mathbf{c}$, dashed is for $\mathbf{E} \| \mathbf{c}$. Note the broad peak at 3365 cm^{-1} that has a component outside of the (001) plane. (**c**) Crustal rutile from other hydrothermal vein and low-grade metamorphic associations: R-6, R-7, R-8. (**d**) Mantle-derived Nb- and Cr-rich rutile from South African kimberlites (Jagersfontein), JAG83-30-3 and JAG85-2.

(1991) determined $\epsilon_{OH} = 3270$ L/(mol·cm²) for a natural rutile sample with 0.09 wt% H_2O as measured by coulommetry. OH concentrations calculated with this value of ϵ_{OH} have an uncertainty of $\pm 20\%$.

The large disparity in the two values of ϵ_{OH} is unexplained. Although both experiments appear to have been carried out with care, we chose to use the molar absorption coefficient of Hammer and Beran (1991) because it was based on a natural sample with an OH absorbance similar to those reported here, and furthermore was based on the actual amount of H_2O released from the rutile on thermal decomposition, and is more in keeping with ϵ_{OH} values recently determined for other minerals (Rossman, 1987). The calculated OH contents of the rutile samples are given in Table 2.

The OH contents of the Nb- and Cr-rich mantle rutile samples are the highest and confirm the finding of similarly high OH content in rutile from a mantle eclogite xenolith by Rossman and Smyth (1990).

Minor components in rutile

The compositions of the rutile samples studied are summarized in Table 3. Natural rutile invariably contains minor components. Minor substitutions in rutile are usually dominated by Fe and V, although Nb, Ta, and Cr may be found in high concentrations (Deer et al., 1962; Putnis and Wilson, 1978; Rumble, 1976; Waychunas, 1991). Rutile samples from xenoliths whose assemblages are believed to record metasomatic processes in the mantle are characterized by higher total impurity concentrations, dominated by Cr and Nb, with distinctly higher concentrations of Zr (Jones et al., 1982; Haggerty, 1983, 1987, 1991; Tollo and Haggerty, 1987).

Discussion of results

H speciation and location in rutile

The polarization of the OH vibration precludes the existence of fluid inclusion or interstitial H_2O in any of our samples. H in rutile therefore is present either as protons bound to structure O or interstitial OH^-. Because the O atoms of rutile are hexagonal closest-packed, the incorporation of interstitial anions is not considered likely; thus the dominant species must be protons bonded to structure oxide ions. The fundamental OH vibrational band in rutile is shifted to lower wavenumbers relative

Table 3. Chemical compositions of rutile samples on the basis of two O atoms

Sample	*n*	Mg	Al	Ti	V	Cr	Fe	Zr	Nb	Ta	Sum
					Natural						
R-1	3	—	—	0.9873	0.0049	0.0110	0.0100	—	0.0004	—	1.0136
				0.0012	0.0002	0.0003	0.0016		0.0001		0.0031
R-2	3	—	—	0.9893	0.0040	0.0004	0.0088	—	0.0005	—	1.0030
				0.0012	0.0013	0.0001	0.0017		0.0001		0.0043
R-4	3	—	0.0002	0.9773	0.0017	—	0.0087	—	0.0110	—	0.9991
			0.0001	0.0073	0.0002		0.0018		0.0041		0.0135
R-5	3	—	0.0003	0.9853	0.0036	0.0004	0.0107	—	0.0025	—	1.0028
			0.0001	0.0005	0.0001	0.0001	0.0001		0.0002		0.0010
R-6	3	—	—	0.9908	0.0008	—	0.0095	—	0.0008	—	1.0019
				0.0010	0.0001		0.0004		0.0002		0.0020
R-7	3	—	0.0002	0.9813	0.0023	0.0030	0.0157	—	0.0022	—	1.0046
			0.0001	0.0005	0.0001	0.0009	0.0003		0.0004		0.0021
R-8	3	—	—	0.9930	0.0015	0.0005	0.0068	—	0.0003	—	1.0020
				0.0001	0.0001	0.0001	0.0005		0.0001		0.0009
JAG83-30-1	1	0.0024	0.0008	0.9110	0.0020	0.0669	0.0046	0.0043	0.0200	0.0021	1.0140
JAG83-30-2	1	—	0.0012	0.9170	0.0022	0.0623	0.0018	0.0042	0.0202	0.0019	1.0109
JAG83-30-3	1	0.0022	0.0036	0.8830	0.0021	0.0924	0.0148	0.0044	0.0194	0.0021	1.0240
JAG85-2	4	0.0012	0.0009	0.9155	0.0022	0.0572	0.0115	0.0040	0.0195	0.0010	1.0130
		0.0008	0.0002	0.0008	0.0002	0.0054	0.0048	0.0001	0.0001	0.0002	0.0123
					Synthetic						
Pure	3	—	—	1.0000	—	—	—	—	—	—	1.0000
				0.0001							0.0001
Al-doped	3	—	0.0005	0.9993	—	—	—	—	—	—	0.9998
			0.0001	0.0005							0.0005

Note: compositions calculated from electron microprobe analyses; — = below detection limit; Na, Ca, Mn, and Si were also analyzed for but not detected. Second rows indicate standard deviation for replicate analyses of the same crystal.

to the isolated OH^- stretch (~3735 cm^{-1}), due to H bonding, and the shift corresponds to an OH···O distance of ~0.28 nm (Nakamoto et al., 1955). The constraint placed on the OH dipole orientation by the polarized spectra limits the possible location of H to only two nonequivalent sites, ½½0 and ½00. The O-O distances across these sites are 0.2533 and 0.3328 nm, respectively (Baur, 1956; Meagher and Lager, 1979; Sugiyama and Takéuchi, 1991). This suggests that the ½½O site (Fig. 1b) is the more likely location for H, and this was confirmed by the study of Swope et al. (1992).

The Al-associated OH peak is present in both the pure and Al-doped synthetic crystals, but there is no impurity-associated peak in Fe-doped rutile (Fig. 2a). As Johnson et al. (1968) pointed out, either there is no association between Fe and H or the resulting shift is too small to be resolved.

Hammer and Beran (1991) regarded the presence of the satellite peak as an indication of formation at high temperature, since it was observed in rutile from mafic pegmatites (3360 cm^{-1}), as well as from eclogite and blueschist (3320 cm^{-1}), and was also observed by Rossman and Smyth (1990) in mantle eclogites. In light of the foregoing discussion, this interpretation is not necessarily correct. The peak at 3320 cm^{-1} is ascribed to Al-associated OH groups, and this conclusion is supported by the relatively high concentration of Al_2O_3 in the Dora Maira eclogitic rutile (0.21 wt%) of Hammer and Beran (1991) and the eclogite xenolith rutile (0.68 wt%) of Rossman and Smyth (1990). The satellite peak at 3360 cm^{-1} found in rutile from mafic pegmatites is also likely to be due to minor element-associated OH, possibly with Mg for which ν_{OH} = 3350 cm^{-1} in synthetic rutile (Johnson et al., 1968). Unfortunately this cannot be confirmed because Mg concentrations were not reported in Hammer and Beran's (1991) study.

The satellite peak at 3360 cm^{-1} in the spectra of R-1 and R-2 (Fig. 2b) is not likely to be due to Mg-associated OH, as the Mg content of these samples is too low (Table 3). The polarization dependence of the absorption bands, however, suggest that part of the H in this sample may be located at the ½O¼ site, which is a distorted tetrahedral site in the channels of the rutile structure (Johnson et al., 1968). This is to our knowledge the first report of OH vibrations not in the (001) plane of rutile and may reflect specific physiochemical conditions encountered in the formation of the aluminum silicate + rutile + lazulite association (Geijer, 1963).

In attempting to understand the crystal chemistry of H in rutile, important constraints are placed on possible H incorporation reactions by the requirement of electroneutrality. Point defects that may be compensated by interstitial protons include Ti vacancies and trivalent or divalent cation substitution. On the other hand, there may also be defects that compete with interstitial H in charge compensation. These include pentavalent cation substitutions, interstitial cations, including Ti^{4+}, and anion vacancies. For the purposes of the present discussion, we will not consider intrinsic defects in assessing charge-coupled compensation mechanisms of H incorporation be-

cause the minor component concentrations in natural rutile are much higher than intrinsic point defect (i.e., Ti and/or O vacancy, Ti interstitial) concentrations.

Oxidation states and sites occupied by minor components in rutile

In deducing plausible reactions for H incorporation based on the electroneutrality condition, constraints regarding the valence states and sites occupied by minor components in rutile are required.

Al. Stebbins et al. (1989), in an ^{27}Al NMR study of Al-doped rutile, concluded that only substitutional Al^{3+} was present. Infrared spectra and electron microprobe analysis of a slice from the same boule of Al-doped rutile used by Stebbins et al. (Al-doped, their Table 5) indicates that OH groups compensate the substitutional Al ions.

V. ESR signals of synthetic V-doped rutile have been interpreted as being due to substitutional V^{4+} (Gerritsen and Lewis, 1960) as well as interstitial V^{4+} (Kubec and Šroubek, 1972), depending on the quenching conditions. Although V^{3+} possesses two unpaired electrons, it is usually difficult to detect by ESR. Therefore, the absence of a V^{3+} ESR signal does not necessarily imply the absence of this cation. H insertion compounds of VO_2 (rutile structure), with the general stoichiometry H_xVO_2, have recently been synthesized by Chippindale et al. (1991). For compounds with $x < 0.08$, no change in XRD-based structure is observed, implying partial reduction of V^{4+} to V^{3+}, concomitant with H insertion. Furthermore, Chavenas et al. (1973) have synthesized VOOH in an orthorhombic modification of the rutile structure, with H ions at displaced ½00 sites of the unit cell. V in rutile-type structures may therefore occur in the trivalent or tetravalent state.

Cr. Gerritsen et al. (1959, 1960) attributed the ESR spectrum of Cr-doped rutile to substitutional Cr^{3+} ions. Ishida et al. (1990) combined ESCA, ESR, and diffuse reflectance spectroscopies to study the oxidation states of Cr in rutile and found predominantly Cr^{3+}, as well as minor Cr^{4+}, incorporated in the structure, the latter only at higher Cr concentrations. Chavenas et al. (1973), in addition to VOOH, synthesized CrOOH with the modified rutile structure. In light of these studies, the trivalent substituting cation is expected to be the dominant form of Cr in natural rutile.

Fe. There are numerous studies dealing with the oxidation state of Fe in synthetic rutile. As with the VOOH and CrOOH, Chavenas et al. (1973) synthesized FeOOH in the modified rutile structure. ESR (Carter and Okaya, 1960; Andersson et al., 1973; Ohlsen and Shen, 1974) and Mössbauer (Nicholson and Burns, 1963; Alam et al., 1966; Stampfl et al., 1973; Sandin et al., 1976; Yamarkin et al., 1978) spectra of synthetic Fe-doped rutile consistently indicate that the dopant is predominantly Fe^{3+} and occupies normal Ti sites. In contrast, wet chemical analyses of Fe-bearing rutile reported by Henriques (1963) indicate that Fe^{2+} predominates in some natural samples.

UV-visible spectra of the samples in Table 1 show no evidence of Fe^{2+}. Preliminary X-ray absorption studies of samples R-1 and R-7 indicate that Fe in these samples is predominantly trivalent, but in JAG85-2, near-edge features indicate both trivalent and divalent Fe (Waychunas, personal communication).

Nb and Ta. Khodos et al. (1988) synthesized rutile solid solutions at 1400 °C with up to 25 mol% $NbO_{2.5}$ but concluded on the basis of inversion voltammetric studies that above ~3 mol% $NbO_{2.5}$ Nb^{5+} is partly reduced to Nb^{4+} and the more Nb-rich compositions should be regarded as NbO_2-TiO_2 solutions with the rutile structure. These results are in agreement with results from ESR studies (Chester, 1961) and recent X-ray absorption spectroscopic investigations of TiO_2-NbO_2 solid solutions, which indicate that with decreasing mole fraction of NbO_2, the Nb^{5+}/Nb^{4+} ratio increases (Antonio et al., 1991). An EXAFS analysis carried out by the latter further indicates that the average Nb-O distance decreases approximately linearly with decreasing Nb concentration and suggests that an increasing fraction of Nb ions occupy tetrahedral interstitial sites with decreasing Nb/(Nb + Ti). The conclusion that may be drawn from studies concerning Nb coordination and oxidation state in rutile is that Nb predominantly occupies normal Ti sites, although it can be tetravalent or pentavalent. Because of a paucity of information about Ta in rutile, however, it is assumed that, like Nb, Ta^{5+} occupies substitutional sites.

Extent of substitution by minor components in rutile

The applicability of a charge compensation model in linking the H content of rutile to the thermodynamic conditions of H trapping requires that the minor components be in homogeneous solid solution in rutile and not in extended defects such as crystallographic shear (CS) structures or exsolved phases.

CS structures occur in synthetic reduced rutile TiO_{2-x} (Hyde, 1976, and references therein), rutile with high concentrations of trivalent impurities such as Fe, Cr, V, Ga, and in natural rutile (Banfield and Veblen, 1991). The normal rutile structure consists of strings of edge-shared $[TiO_6]$ octahedra (parallel to **c**) in two mutually perpendicular orientations and joined by corner sharing. Progressive reduction of Ti^{4+} or the introduction of trivalent impurities induces the formation of oriented planar defects with the hematite structure and results in a homologous series of related structures, termed Magnéli phases, $(Ti,M)_nO_{2n-1}$, with n depending on the CS plane density.

Experimental phase equilibria at 0.1 MPa in the systems $AlO_{1.5}$-TiO_2, $CrO_{1.5}$-TiO_2, $VO_{1.5}$-TiO_2, $NbO_{2.5}$-TiO_2, $TaO_{2.5}$-TiO_2, and FeO-$FeO_{1.5}$-TiO_2 indicate that the compositions of our rutile samples are generally within the rutile single-phase field (Brach et al., 1977; Bursill and Jun, 1984; Khodos et al., 1988; MacChesney and Muan, 1959; Mertin et al., 1970; O'Keefe and Ribble, 1972; Roth and Coughanour, 1955; Slepetys and Vaughan, 1969; Taylor, 1964; Webster and Bright, 1961; Wittke, 1967;

Woerman et al., 1969). In addition, HRTEM images of samples R-6 and JAG85-2 (J. Banfield, personal communication) show no evidence of CS structures initially, although annealing under the electron beam resulted in exsolution of hematite structure platelets rich in Cr and Fe in sample JAG85-2, similar to the phenomenon reported by Putnis (1978). Furthermore, the effect of the minor components on the unit-cell dimensions of sample JAG85-2 is such that a is expanded ($a = 0.46029 \pm 23$ nm) compared with the value for pure TiO_2 ($a = 0.45935 \pm 19$), as would be expected for a substitutional solid solution.

H and its relation to minor components in rutile

Following the arguments and evidence presented in the preceding sections, it would seem reasonable to assign the minor components to substitutional sites, with oxidation states of 3+ for Cr, Fe, V, and Al, 2+ for Mg, and 5+ for Nb and Ta. Coupled substitutions of the type $M^{3+} + M^{5+} \leftrightarrow 2Ti^{4+}$ and $M^{2+} + 2M^{5+} \leftrightarrow 3Ti^{4+}$ are required to maintain electroneutrality. There is evidence for such charge-coupled substitution in rutile, and there are several Ti-free oxide end-members that have been synthesized or found in nature. In the absence of H interstitials, the charge balance in rutile is

$$[Cr^{3+}]_{Ti} + [Fe^{3+}]_{Ti} + [V^{3+}]_{Ti} + [Al^{3+}]_{Ti} + 2[Mg^{2+}]_{Ti} = [Nb^{5+}]_{Ti} + [Ta^{5+}]_{Ti} \quad (1)$$

where $[M]_{Ti}$ represents the mole fraction of M at Ti sites.

Figure 3 illustrates the covariation of minor element concentrations in natural rutile from a wide variety of environments, including samples analyzed in the present work and analyses found in the literature. There is generally an excess of trivalent impurities over pentavalent per formula unit, which is presumably compensated by H^+ interstitials (Fig. 3). If this is the dominant incorporation mechanism for H in rutile, a one-to-one correlation between the calculated charge deficit per formula unit and the concentration of H per formula unit is expected:

$$[H^+] = \Sigma[M^{3+}]_{Ti} + 2\Sigma[M^{2+}]_{Ti} - \Sigma[M^{5+}]_{Ti}. \quad (2)$$

Figure 4 supports this hypothesis, although there is considerable scatter in the correlation. The scatter may result partly from substitutional cations in multiple oxidation states (Fe, and possibly V, Nb). Calculation of a unique distribution of cation oxidation states is not possible, however, from the microprobe data alone. The effect of the assumed oxidation state of an impurity on the calculated charge deficit, however, is obvious. For example, if any Fe is present as Fe^{2+} or any Nb is tetravalent, then the charge deficit per formula unit will be underestimated by Equation 2. On the other hand, if any V is tetravalent, the charge deficit per formula unit will be overestimated. The result of assuming all Fe to be Fe^{3+} vs. Fe^{2+} is shown in Figure 4. It is interesting to note that for sample R-4 (Magnet Cove), the charge balance is satisfied only if all Fe is taken as divalent (Table 3). This is in agreement with wet chemical analyses of Magnet Cove rutile reported by Henriques (1963).

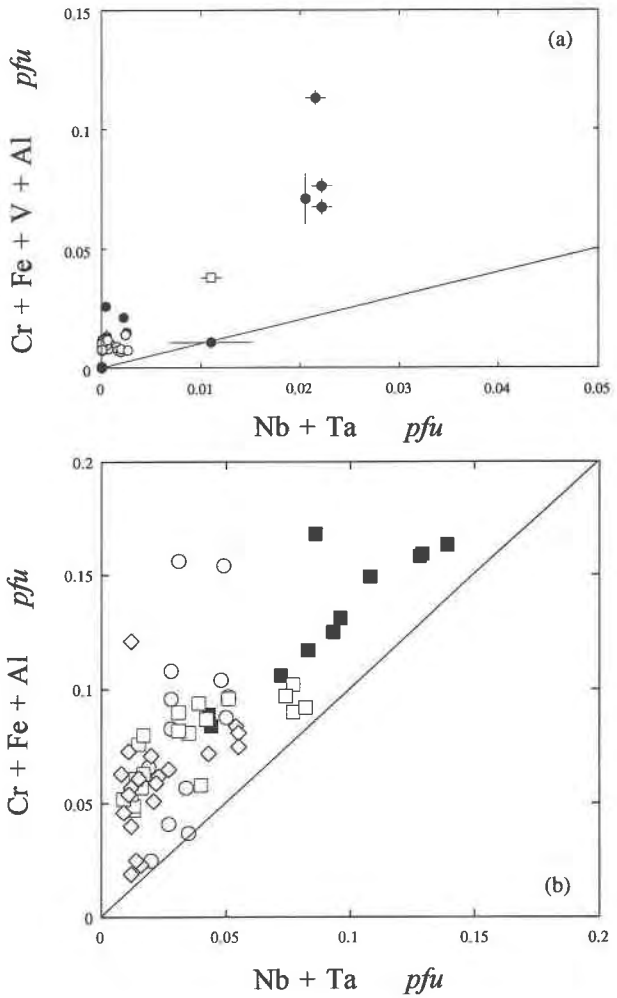

Fig. 3. (**a**) Correlation between Cr + Fe + V + Al and Nb + Ta contents in rutile. The line represents the trend expected for the charge-coupled substitution $M^{3+} + M^{5+} = 2Ti^{4+}$. Solid circles are from the present study, open circles are data from Hammer and Beran (1991), and the square is from Rossman and Smyth (1990). In general, natural rutile exhibits an excess of trivalent over pentavalent substitutional cations. (**b**) Similar plot for Nb- and Cr-rich rutile from upper-mantle xenolith suites from South African kimberlites. The solid line defines the expected trend for charge-coupled substitution as in **a**. Solid squares are for rutile associated with ilmenite from Orapa. Open symbols are for samples from Jagersfontein: squares = rutile associated with ilmenite; circles = rutile associated with lindsleyite mathiasite; diamonds = rutile associated with armalcolite [data from Tollo and Haggerty (1987) and Haggerty (unpublished analyses)].

Despite the scatter in Figure 4, an assessment of the validity of our choice of ϵ_{OH} in rutile can be made. The H contents calculated using ϵ_{OH} of Johnson et al. (1973) would be approximately one-fifth of the values reported in Table 2. The H contents calculated with Hammer and

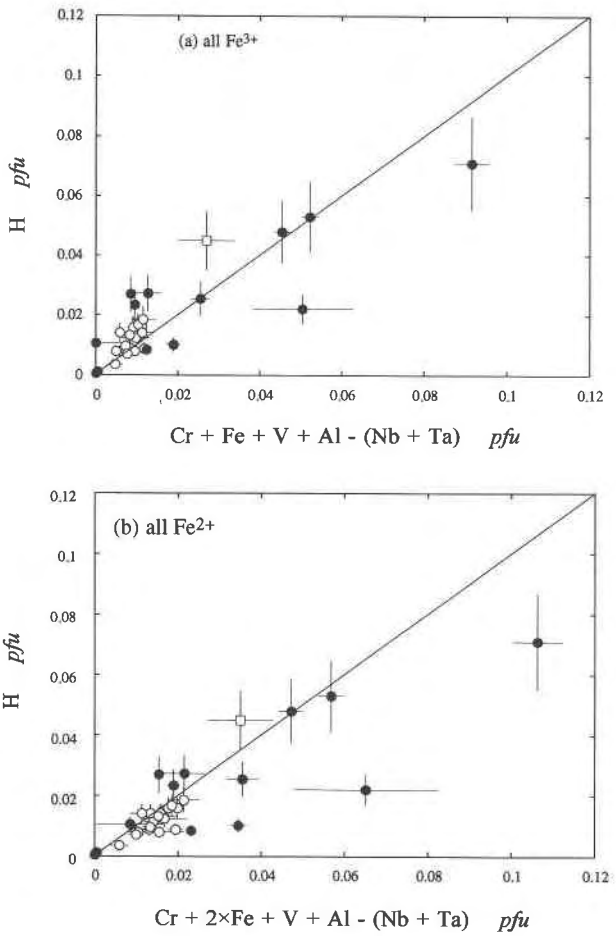

Fig. 4. H content vs. calculated charge deficiency. Symbols as in Fig. 3a. Solid line represents expected trend for 1:1 compensation of calculated charge deficiency by interstitial protons. (a) Charge deficiency calculated assuming all Fe is Fe^{3+}. (b) Charge deficiency calculated assuming all Fe is Fe^{2+}. Within the range of uncertainty in oxidation state of Fe, most of the samples fall around a 1:1 relation between H content and calculated charge deficiency.

Beran's (1991) ϵ_{OH} are clearly in better accord with the expected correlation with minor elements.

Application of the H content in rutile as a geohygrometer

Because of its affinity for H incorporation, rutile may be of use as an indicator of the fugacity or activity of H_2O accompanying geologic processes. In principle, this requires the formulation of a thermodynamic model based on the relations found between H content and minor component concentrations, taking into account the various reactions and electroneutrality constraints. To make such a geohygrometer useful, experimental calibration of the effects of pressure, temperature, O-H species fugacity, and composition would then be necessary.

Consider a simple hypothetical situation, the coexistence of rutile with hematite, at equilibrium with a hydrous vapor phase. At 0.1 MPa the two phases coexist stably below ~585 °C and f_{O_2} at or above that defined by hematite-magnetite coexistence (Anovitz et al., 1985). At a given pressure, temperature, and f_{O_2} where the two phases are in equilibrium, a nonstoichiometric solid solution of the hematite component in rutile $(Fe_{2x}Ti_{1-2x})O_{2-x}$ will exist. The substitution of Ti^{4+} by Fe^{3+} requires compensation, in this case by an intrinsic point defect. Although the intrinsic point defect structure of rutile is by no means well understood, O vacancies are believed to predominate under relatively oxidizing conditions (Millot et al., 1987, and references therein), although local reconstruction of the structure in the vicinity of the anion vacancy may occur (Bursill and Blanchin, 1984). The solid solution of Fe_2O_3 in rutile in the absence of H_2O may thus be described by

$$Fe_2O_{3(hem)} \longleftrightarrow 2Fe^{3+}_{Ti} + 3O^{2-}_{O} + V_O \qquad (3a)$$

or

$$Fe_2O_{3(hem)} \longleftrightarrow 2FeO_{1.5(rut)} + V_{O(rut)} \qquad (3b)$$

where $V_{O(rut)}$ is a doubly ionized anion vacancy and the subscripts on the right side in Equation 3a refer to rutile structure sites. With the assumption of ideal behavior for low defect concentrations, the equilibrium for this reaction is

$$K_4(P, T, f_{O_2}) = X[FeO_{1.5(rut)}]^2 \cdot x \qquad (4)$$

where $X[FeO_{1.5(rut)}]$ is the mole fraction of $FeO_{1.5}$ in rutile and x is the departure from stoichiometry due to anion vacancies in rutile $(Ti_{1-2x}Fe_{2x})O_{2-x}$. At constant pressure, temperature, and f_{O_2} in the dry system, the solubility of $FeO_{1.5}$ in rutile is fixed. In the presence of a hydrous vapor, however, the incorporation of H_2O and formation of interstitial H^+ in rutile may be written

$$H_2O_{(v)} \leftrightarrow 2H^+_i + O^{2-}_O. \qquad (5)$$

The interstitial protons can compensate substitutional Fe^{3+} and the oxide ion can fill the anion vacancies created by the nonstoichiometric solid solution to maintain neutrality in the crystal. By combining Equations 3 and 5, the solubility of hematite in rutile in the presence of H_2O can then be described as

$$Fe_2O_{3(hem)} + H_2O_{(v)} \leftrightarrow 2HFeO_{2(rut)} \qquad (6)$$

for which the equilibrium constant may be expressed

$$K_6(P, T, f_{O_2}) = \frac{X[HFeO_{2(rut)}]^2}{f_{H_2O}}. \qquad (7)$$

Keeping in mind that $X[HFeO_{2(rut)}]$ is equal to the H content per formula unit as determined from IR measurements, Equation 7 can be rearranged to give

$$H\ (pfu) = [K_6(P, T, f_{O_2}) \cdot f_{H_2O}]^{1/2}. \qquad (8)$$

Therefore, the H content of rutile is proportional to the square root of f_{H_2O} in the vapor phase with which it is equilibrated. At high f_{H_2O}, rutile may eventually reach

saturation with respect to the FeOOH component, thus reaching an upper limit to both the H and Fe concentrations in rutile.

Applicability of such a geohygrometer to real systems, however, is complicated, requiring a more elaborate treatment taking into account the various minor components. For a given rutile-bearing assemblage, f_{H_2O} could in principle be estimated if independent constraints on T, P, and f_{O_2} are available and the T, P, and composition dependence of K_6 is known.

Potential problems in applying this geohygrometer to natural systems may arise in establishing whether the P and T determined by thermobarometry are the same as that under which rutile last equilibrated with a hydrous phase. In light of the fact that protons diffuse much faster through rutile than any of the minor cations present (Kingsbury et al., 1968; Hoshino et al., 1985; Sasaki et al., 1985), the H content will essentially be fixed below temperatures at which minor component diffusion becomes negligible. The temperatures at which H becomes fixed depend on the cation in question, but for most transition metals diffusion becomes insignificant below ~500 °C. Complications may also arise from postentrapment modification of the H content caused by reduction or oxidation of Fe, V, or Nb, but this problem may be overcome by examination of the compositional systematics in a suite of samples from the same occurrence.

Some qualitative conclusions can nevertheless be drawn from a comparison of H content and the calculated charge deficiency in specific samples. At relatively low values of f_{H_2O}, intrinsic species are the dominant charge-compensating defects, and this should result in H contents that are less than those predicted by Equation 2. At relatively high values of f_{H_2O}, on the other hand, H contents should be closely predicted by Equation 2.

H in Nb- and Cr-rich rutile from upper mantle xenoliths

A rigorous thermodynamic treatment of H in rutile is beyond our present scope, particularly as regards the essentially unknown effects of pressure on H and minor element incorporation. The systematics among the upper mantle rutile values plotted in Figure 4 allow some inferences to be made. The H contents of JAG83-30 and the Roberts Victor eclogite rutile of Rossman and Smyth (1990) closely match the calculated charge deficiency per formula unit, whereas the H content of JAG85-2 is significantly less than required for charge balance. From the foregoing model of H incorporation in rutile, the limited data presented here strongly suggest the presence of a hydrous fluid phase and perhaps local variability in f_{H_2O} in the upper mantle during or after the formation of Nb- and Cr-rich rutile. This is consistent with and supports the interpretations of Haggerty (1987) for the origin of Nb- and Cr-rich rutile and other incompatible element enriched titanates in upper mantle xenoliths as the product of metasomatism by a fluid phase or melt rich in hydrous incompatible elements.

The storage of small amounts of H in the mantle in nominally anhydrous minerals was proposed by Martin and Donnay (1972), and our present state of knowledge is summarized by Bell and Rossman (1992). The relative importance of a given mineral as regards the H budget of the mantle will obviously depend on the amount of H that can be accommodated in the phase and its distribution and concentration in the mantle.

The H contents in mantle-derived rutile (Table 2) are among the highest reported for nominally anhydrous minerals (Rossman, 1987; Bell and Rossman, 1992). Rutile, although a common phase, is believed to be present in the mantle only at accessory levels (Haggerty, 1983, 1987, 1991; Tollo and Haggerty, 1987; Rossman and Smyth, 1990). Therefore, despite the fact that rutile has a very great affinity for H incorporation, it is not expected to be a significant mantle H_2O repository, except possibly on a very small scale, in regions of rutile-dominated assemblages such as the rutile-ilmenite and rutile-silicate nodules reported from Jagersfontein, Orapa, and other localities (Ottenburgs and Fieremans, 1979; Haggerty, 1983, 1987; Tollo and Haggerty, 1987; Schulze, 1990).

The high H content of mantle-derived rutile may also have implications for mantle silicate mineral relations, on the grounds that stishovite, the SiO_2 modification isomorphous with rutile, may occur in the mantle transition zone as the result of incongruent pressure-induced phase transformations of orthopyroxene to β spinel or γ spinel structures that require the stoichiometric release of SiO_2 as stishovite (Fei et al., 1990; Gasparik, 1990).

Acknowledgments

We would like to extend our appreciation to Ulrich Klabunde (E.I. du Pont de Nemours and Company, Inc.) for providing the synthetic samples and stimulating discussions and to J.L. Rosenfeld for a natural sample (R-8). We also thank Jill Banfield (University of Wisconsin, Madison) for her interest in this study and for access to data prior to publication, Glenn Waychunas (Stanford University) for contributions from XAS that significantly constrained our interpretations, and David Bell for performing the microprobe analyses and discussions. Helpful comments were provided by Harry Green and Alison Pawley. The research was funded in part by NSF grants EAR-91-04059 to G.R.R. and EAR-91-16551 to S.E.H. Division contribution no. 5284.

References cited

Alam, M., Chandra, S., and Hoy, G.R. (1966) Mössbauer studies of spin relaxation of Fe^{3+} in TiO_2. Physics Letters, 22, 26–28.

Andersson, P-O., Kollberg, E.L., and Jelenski, A. (1973) Extra EPR spectra of iron-doped rutile. Physical Reviews, B8, 4956–4965.

——— (1974) Charge compensation in iron-doped rutile. Journal of Physics C: Solid State Physics, 7, 1868–1880.

Anovitz, L.M., Treiman, A.H., Essene, E.J., Hemingway, B.S., Westrum, E.F., Jr., Wall, V.J., Burriel, R., and Bohlen, S.R. (1985) The heat capacity of ilmenite and phase equilibria in the system Fe-Ti-O. Geochimica et Cosmochimica Acta, 49, 2027–2040.

Antonio, M.R., Song, I., and Yamada, H. (1991) Coordination and valence of niobium in TiO_2-NbO_2 solid solutions through X-ray absorption spectroscopy. Journal of Solid State Chemistry, 93, 183–192.

Banfield, J.F., and Veblen, D.R. (1991) The structure and origin of Fe-bearing platelets in metamorphic rutile. American Mineralogist, 76, 113–127.

Baur, W.H. (1956) Über die Verfeinerung der Kristallstrukturbestimmung

einiger Vertreter des Rutiltyps: TiO_2, SnO_2, GeO_2 und MgF_2. Acta Crystallographica, 9, 515–520.

Bell, D.R., and Rossman, G.R. (1992) Water in the earth's mantle: The role of nominally anhydrous minerals. Science, 255, 1391–1397.

Beran, A., and Zemann, J. (1971) Measurement of the infrared-pleochroism in minerals. XI. The pleochroism of the OH-stretching frequency in rutile, anatase, brookite, and cassiterite. Tschermaks mineralogisch-petrographische Mitteilungen, 15, 71–80.

Brach, B., Grey, I.E., and Li, C. (1977) Phase equilibria in the system V_2O_3-Ti_2O_3-TiO_2 at 1473 K. Journal of Solid State Chemistry, 20, 29–41.

Bursill, L.A., and Blanchin, M.G. (1984) Structure of small oxygen vacancy defects in nonstoichiometric rutile. Journal of Solid State Chemistry, 51, 321–335.

Bursill, L. A., and Jun, S.G. (1984) Temperature dependence of the solubility limit of chromia (Cr_2O_3) in titania (TiO_2). Journal of Solid State Chemistry, 51, 388–395.

Carter, D.L., and Okaya, A. (1960) Electron paramagnetic resonance in Fe^{3+} in TiO_2 (rutile). Physical Reviews, 118, 1485–1490.

Chavenas, J., Joubert, J.C., Capponi, J.J., and Marézio, M. (1973) Synthèse de nouvelles phases denses d'oxyhydroxydes $M^{3+}OOH$ des métaux de la première série de transition, en milieu hydrothermal à très haute pression. Journal of Solid State Chemistry, 6, 1–15.

Chester, P.F. (1961) Cross-doping agents for rutile masers. Journal of Applied Physics, 32, 866–868.

Chippindale, A.M., Dickens, P.G., and Powell, A.V. (1991) Synthesis, characterization and inelastic neutron scattering study of hydrogen insertion compounds of VO_2 (rutile). Journal of Solid State Chemistry, 93, 526–533.

Deer, W.A., Howie, R.A., and Zussman, J. (1962) An introduction to rock-forming minerals, 528 p. Longmans, London.

Fei, Y., Saxena, S.K., and Navrotsky, A. (1990) Internally consistent thermodynamic data and equilibrium phase relations for compounds in the system MgO-SiO_2 at high pressure and high temperature. Journal of Geophysical Research, 95, 6915–6928.

Gasparik, T. (1990) Phase relations in the transition zone. Journal of Geophysical Research, 95, 15751–15769.

Geijer, P. (1963) Genetic relationships of the paragenesis Al_2SiO_5-lazulite-rutile. Arkiv für Mineralogie und Geologie, 3, 423–464.

Gerritsen, H.J., and Lewis, H.R. (1960) Paramagnetic resonance of V^{4+} in TiO_2. Physical Reviews, 119, 1010–1012.

Gerritsen, H.J., Harrison, S.E., Lewis, H.R., and Wittke, J.P. (1959) Fine structure, hyperfine structure, and relaxation times of Cr^{3+} in TiO_2 (rutile). Physical Review Letters, 2, 153–155.

Gerritsen, H.J., Harrison, S.E., and Lewis, H.R. (1960) Chromium-doped titania as a maser material. Journal of Applied Physics, 31, 1566–1571.

Haggerty, S.E. (1983) The mineral chemistry of new titanates from the Jagersfontein kimberlite, South Africa: Implications for metasomatism in the upper mantle. Geochimica et Cosmochimica Acta, 47, 1833–1854.

——— (1987) Metasomatic mineral titanates in upper mantle xenoliths. In P.H. Nixon, Ed., Mantle xenoliths, p. 671–690. Wiley, New York.

——— (1991) Oxide mineralogy of the upper mantle. In Mineralogical Society of America Reviews in Mineralogy, 25, 355–416.

Hammer, V.M.F., and Beran, A. (1991) Variations in the OH concentration of rutiles from different geological environments. Mineralogy and Petrology, 45, 1–9.

Henriques, A. (1963) Ferriferous rutile and ferriferous cassiterite. Arkiv für Mineralogie und Geologie, 3, 385–394.

Hill, G.J. (1968) The effect of hydrogen on the electrical properties of rutile. British Journal of Applied Physics, 1, 1151–1162.

Hoshino, K., Peterson, N.L., and Wiley, C.L. (1985) Diffusion and point defects in TiO_{2-x}. Journal of Physics and Chemistry of Solids, 46, 1397–1411.

Hyde, B.G. (1976) Rutile: Planar defects and derived structures. In H.-R. Wenk, Ed., Electron microscopy in mineralogy, 564 p. Springer-Verlag, New York.

Ishida, S., Hayashi, M., Fujimura, Y., and Fujiyoshi, K. (1990) Spectroscopic study of the chemical state and coloration of chromium in rutile. Journal of the American Ceramic Society, 73, 3351–3355.

Johnson, O.W., Ohlsen, W.D., and Kingsbury, P.I. (1968) Defects in rutile. III. Optical and electrical properties of impurities and charge carriers. Physical Reviews, 175, 1102–1109.

Johnson, O.W., DeFord, J., and Shaner, J.W. (1973) Experimental technique for the precise determination of H and D concentration in rutile (TiO_2). Journal of Applied Physics, 44, 3008–3012.

Johnson, O.W., Paek, S.-H., and DeFord, J.W. (1975) Diffusion of H and D in TiO_2. Suppression of internal fields by isotope exchange. Journal of Applied Physics, 46, 1026–1033.

Jones, A.P., Smith, J.V. and Dawson, J.B. (1982) Mantle metasomatism in 14 veined peridotites from Bultfontein mine, South Africa. Journal of Geology, 90, 435–453.

Khodos, M.Y., Belysheva, G.M., and Krivosheev, N.V. (1988) Solid solutions with the rutile structure in the TiO_2-Nb_2O_5 system. Russian Journal of Inorganic Chemistry, 33, 604–606.

Kingsbury, P.I., Ohlsen, W.D., and Johnson, O.W. (1968) Defects in rutile. II. Diffusion of interstitial ions. Physical Reviews, 175, 1098–1101.

Kubec, F., and Šroubek, Z. (1972) Paramagnetic resonance of interstitial V^{4+} in TiO_2. Journal of Chemical Physics, 57, 1660–1663.

MacChesney, J.B., and Muan, A. (1959) Studies in the system iron oxide-titanium dioxide. American Mineralogist, 44, 926–945.

Martin, R.F., and Donnay, G. (1972) Hydroxyl in the mantle. American Mineralogist, 57, 554–570.

Meagher, E.P., and Lager, G.A. (1979) Polyhedral thermal expansion in the TiO_2 polymorphs: Refinement of the crystal structures of rutile and brookite at high temperature. Canadian Mineralogist, 17, 77–85.

Mertin, W., Gruehn, R., and Schäfer, H. (1970) Neue Beobachtungen zum System TiO_2-Ta_2O_5. Journal of Solid State Chemistry, 1, 425–444.

Millot, F., Blanchin, M-G., Tetot, R., Marucco, J-F., Poumellec, B., Picard, C., and Touzelin, B. (1987) High temperature non-stoichiometric rutile TiO_{2-x}. Progress in Solid State Chemistry, 17, 263–293.

Nakamoto, K., Margoshes, M., and Rundle, R.E. (1955) Stretching frequencies as a function of distances in hydrogen bonds. Journal of the American Chemical Society, 77, 6480–6486.

Nicholson, W.J., and Burns, G. (1963) Spin Hamiltonian parameter D versus axial crystal field for S-state ions. Physical Reviews, 129, 2490–2495.

Ohlsen, W.D., and Shen, L.N. (1974) Hyperfine structure of Fe^{3+} ions in rutile (TiO_2). Journal of the Physical Society of Japan, 37, 1467.

O'Keefe, M., and Ribble, T.J. (1972) Interdiffusion and the solubility limits of Cr_2O_3 in the rutile phase of TiO_2. Journal of Solid State Chemistry, 4, 351–356.

Ottenburgs, R., and Fieremans, M. (1979) Rutile-silicate intergrowths from the kimberlite formations at Mguji-Mayi (Bakwanga, Zaire). Bulletin de la Société Belge de Géologie, 3, 197–203.

Putnis, A. (1978) The mechanism of exsolution of hematite from iron-bearing rutile. Physics and Chemistry of Minerals, 3, 183–197.

Putnis, A., and Wilson, M.M. (1978) A study of iron-bearing rutiles in the paragenesis TiO_2-Al_2O_3-P_2O_5-SiO_2. Mineralogical Magazine, 42, 255–263.

Rossman, G.R. (1987) Vibrational spectroscopy of hydrous components. In Mineralogical Society of America Reviews in Mineralogy, 18, 193–206.

Rossman, G.R., and Smyth, J.R. (1990) Hydroxyl contents of accessory minerals in mantle eclogites and related rocks. American Mineralogist, 75, 775–780.

Roth, R.S., and Coughanour, L.W. (1955) Phase equilibrium relations in the systems titania-niobia and zirconia-niobia. National Bureau of Standards Journal of Research, 55, 209–213.

Rumble, D. (1976) Oxide minerals in metamorphic rocks. In Mineralogical Society of America Reviews in Mineralogy, 3, R1–R24.

Sandin, T.R., Schroeer, D., and Spencer, C.D. (1976) Mössbauer effect for ^{57}Fe and ^{57}Co in TiO_2 (rutile). Physical Reviews, B13, 4784–4789.

Sasaki, J., Peterson, N.L., and Hoshino, K. (1985) Tracer impurity diffusion in single-crystal rutile (TiO_{2-x}). Journal of Physics and Chemistry of Solids, 46, 1267–1283.

Schulze, D.J. (1990) Silicate-bearing rutile-dominated nodules from South African kimberlites: Metasomatized cumulates. American Mineralogist, 75, 97–104.

Slepetys, R.A., and Vaughan, P.A. (1969) Solid solution of aluminum oxide in rutile titanium dioxide. Journal of Physical Chemistry, 73, 2157–2162.

Soffer, B.H. (1961) Studies of the optical and infrared absorption spectra of rutile single crystals. Journal of Chemical Physics, 35, 940–945.

Stampfl, P.P., Travis, J.C., and Bielefeld, M.J. (1973) Mössbauer spectroscopic studies of iron-doped rutile. Physica Status Solidi, A15, 181–189.

Stebbins, J.F., Farnan, I., and Klabunde, U. (1989) Aluminum in rutile (TiO_2): Characterization by single-crystal and magic-angle-spinning nuclear magnetic resonance. Journal of the American Ceramic Society, 72, 2198–2200.

Sugiyama, K., and Takéuchi, Y. (1991) The crystal structure of rutile as a function of temperature up to 1600°C. Zeitschrift für Kristallographie, 194, 305–313.

Swope, R.J., Smyth, J.R., and Larson, A.C. (1992) Crystal chemistry of hydrogen in rutile of mantle origin (abs.). Eos, 73, 651.

Taylor, R.W. (1964) Phase equilibria in the system FeO-Fe_2O_3-TiO_2 at 1300°C. American Mineralogist, 49, 1016–1030.

Tollo, R.P., and Haggerty, S.E. (1987) Nb-Cr rutile in the Orapa kimberlite, Botswana. Canadian Mineralogist, 25, 251–264.

von Hippel, A., Kalnajs, J., and Westphal, W.B. (1962) Protons, dipoles and charge carriers in rutile. Journal of Physics and Chemistry of Solids, 23, 779–799.

Waychunas, G.A. (1991) Crystal chemistry of oxides and oxyhydroxides. In Mineralogical Society of America Reviews in Mineralogy, 25, 11–68.

Webster, A.H., and Bright, N.F.H. (1961) The system iron-titanium-oxygen at 1200°C and oxygen partial pressures between 1 atm and $2 \cdot 10^{-14}$ atm. Journal of the American Ceramic Society, 44, 110–116.

Wittke, J.P. (1967) Solubility of iron in TiO_2 (rutile). Journal of the American Ceramic Society, 50, 586–588.

Woerman, E., Brezny, B., and Muan, A. (1969) Phase equilibria in the system MgO-iron oxide-TiO_2 in air. American Journal of Science, 267-A, 463–479.

Yamarkin, V.K., Teslenko, S.P., and Knyazev, A.I. (1978) Mössbauer study of Sb and Fe impurities in semiconducting and insulating rutile. Physica Status Solidi, A45, 63–69.

Manuscript received November 2, 1992
Manuscript accepted July 18, 1993